Polymer Chemistry

PAPER

View Article Online
View Journal | View Issue

Cite this: *Polym. Chem.*, 2018, **9**, 1072

Squalene/polyethylenimine based non-viral vectors: synthesis and use in systems for sustained gene release†

Geta David, *[a] Lilia Clima,[b] Manuela Calin,[c] Cristina Ana Constantinescu,[c] Mihaela Balan-Porcarasu, [b] Cristina Mariana Uritu[b,d] and Bogdan C. Simionescu*[a,b]

The design of new non-viral gene vectors and their integration into a biomaterial scaffold are intensively explored nowadays, aimed at developing more efficient gene delivery systems capable of clinical translation. Herein, a series of squalene/branched polyethylenimine (Sq/BPEI) based conjugates were synthesized and their potential in gene delivery, as such or included in a three-dimensional hybrid scaffold (atelocollagen-glycosaminoglycan-polycaprolactone/nano-hydroxyapatite), was investigated. The developed materials were characterized through spectral (^{1}H-NMR, ^{13}C-NMR, FT-IR) and optical (STEM) techniques. The extent and duration of gene expression for the developed systems were monitored using luciferase assays and fluorescence microscopy. All the investigated systems exhibited a high transfection efficiency without or with moderate cytotoxic side effects (MTS assay data). The best results were obtained with the guanidinylated compound Sq-BPEI-G for both simple and combined polyplex/matrix systems. The polyplex delivery from the hybrid matrix was assessed through kinetic studies using a labeled Sq/BPEI conjugate. For the polyplex (Sq/BPEI – DNA plasmid)/3D matrix system, the expression of the delivered plasmids was observed over a 26 day- period. The reported preliminary data recommend the studied biomaterials as possible candidates for the development of a new gene-activated matrix (GAM) platform.

Received 10th October 2017,
Accepted 8th January 2018

DOI: 10.1039/c7py01720k

rsc.li/polymers

1. Introduction

Nowadays, gene therapy is considered as one of the most promising therapeutic approaches for the treatment of many inherited or acquired genetic disorders or diseases. Basically, it consists of replacing or inhibiting the faulty gene in cells by direct transfer of genetic material to cells or tissues, a process involving viral or non-viral vectors and carriers capable of condensing natural or synthetic nucleic acid and overcoming physiological barriers in humans.[1] In an effort to avoid the drawbacks of viral vectors (low stability, safety issues related to immunogenicity and risk of insertional mutagenesis), many investigations have been conducted to obtain new non-viral vectors (easy to prepare and modify, rather stable and safe profile, but usually of lower transfection efficiency as compared to the viral vectors) with improved performances. Lipids, polymers (cationic polymers, conjugated polymers, and biopolymers), hybrids, and inorganics (calcium phosphates, magnetic nanoparticles, quantum dots, carbon nanotubes, and gold nanoparticles) were used as materials, in different forms (pellets, nanoparticles, nanocomposites, 3-D matrices, *etc.*).[2–6] Polycations (particularly polyethylenimine–PEI[7]) and lipid-based structures (cationic liposomes, cationic lipids, cationic solid lipids, and cationic emulsions[3]) are routinely exploited in gene delivery, being easy to produce, non-immunogenic, and non-oncogenic, with good physical and chemical stability (relative facile storage and purification). Primarily, they have the ability to efficiently interact with DNA or plasmid DNA (pDNA) to form nano-sized complexes, a requirement to pass through the cell membrane. Moreover, PEI presents intrinsic endosomolytic activity, while lipid structures can interact with the cell membrane, facilitating cell internalization and increasing gene transfer efficiency. However, they both suffer from a slight risk of toxicity at high-dose applications.[8] For PEI, cytotoxicity is also dependent on chain topology and length, *e.g.*,

[a]*Department of Natural and Synthetic Polymers, "Gh. Asachi" Technical University of Iasi, Iasi 700050, Romania. E-mail: dgeta54@yahoo.com, bcsimion@icmpp.ro; http://orcid.org/0000-0001-6626-5317*
[b]*"Petru Poni" Institute of Macromolecular Chemistry of Romanian Academy, Iasi 700487, Romania*
[c]*Institute of Cellular Biology and Pathology "Nicolae Simionescu" of Romanian Academy, Bucharest 050568, Romania*
[d]*Advanced Research and Development Center in Experimental Medicine, "Gr. T. Popa" University of Medicine and Pharmacy, Iasi 700115, Romania*
†Electronic supplementary information (ESI) available. See DOI: 10.1039/c7py01720k

linear PEI (LPEI) being less cytotoxic than branched PEI (BPEI), while a lower polymerization degree is related at the same time to decreased/no-toxicity and unfortunately, to a decreased transfection efficiency, thus requiring an equilibrated and rational carrier design.

Different strategies have been developed for the optimization of the efficiency of non-viral vectors and improvement of their cytocompatibility, including derivatization, coupling with biodegradable/less toxic compounds, improvement of polyplex preparation methods and delivery techniques.[9]

Aiming to develop small controlled structures with good stability and low toxicity, we present herein the synthesis, characterization and application evaluation of gene-delivery of new amphiphilic squalene/polyethylenimine (Sq/BPEI) based conjugates (Scheme 1). In search for a rational design, the literature data on non-viral gene vector design recommendations[9] and on water soluble lipopolymer advantages (aggregation ability in nanostructures, stability, low toxicity, and increase in transfection efficiency)[10] were analysed. In an earlier paper, we reported the use of squalenoylation[11] and Dynamic Constitutional (DC)[12] approaches to develop and investigate Dynamic Constitutional Frameworks based on squalene, polyethylene glycol (PEG) and PEI components, reversibly connected in a hyperbranched structure, for a deeper understanding of the structure-performance relation (in terms of transfection efficiency and tolerance in humans cells) in such compounds.[13]

The optimal DNA binding and transfection ability of the vectors obtained herein as well as the viability of HeLa and HEK 293T cells in their presence were investigated in contrast with the corresponding naked BPEI. Aimed at the future development of GAM systems, the polyplexes prepared with genetic material were incorporated in a hybrid cryogel, containing biopolymers, poly(ε-caprolactone) and polyethylenimine functionalized nanohydroxyapatite.[14] The performances as well as the polyplexes delivery kinetics were comparatively evaluated for the resultant combined systems. GAMs combine tissue engineering and gene therapy strategies, making them a promising alternative for prolonged and localized release of genetic material, while improving biocompatibility. The technique is considered to be more appropriate in clinical applications–it offers the potential to bypass some extracellular barriers that limit scaling-up possibility and require laborious multiple-step fabrication.[6,15–17] The choice of the components of such a combined system is a real challenge and thus, it is a topical subject of recent research. Their compatibility controls the release profile, while their characteristics highly influence the performances and suitability for application in regeneration of specific tissues.

2. Results and discussion

Sq/BPEI conjugates synthesis and characterization

Specific moieties with appropriate functional linking groups were included in the envisaged conjugate design to fulfill the requirements associated with the known steps of the transfection process (genetic material loading, protection during systemic circulation, binding to and entry into the cells, and intracellular trafficking–endosomal escape, DNA/vector dissociation, and nuclear localization) in order to overcome the related biological barriers.[1–3] Mild preparation conditions–such as room temperature, common solvents or aqueous reaction medium – were preferred (Scheme 1, Experimental section in ESI†). Squalene and BPEI were selected for the efficient compaction of nucleic acids to nano-sized aggregates, promoting their internalization and preventing their nuclease-promoted destruction.[3,5,9] The PEI moiety also confers a buffering (proton sponge) effect, allowing facilitated endosomal escape and improved properties in terms of nuclear localization.[7,9] Considering the cytotoxicity issues,[8] a low molecular weight BPEI (LMWPEI) ($M_w \sim 1.8$ kDa) was used. Bioconjugation of LMWPEIs with lipids was proved to enhance transfection efficiency by improvement of nucleic acid condensation (self-assembling capacity of a lipid moiety favoring the required cationic charge accumulation) and of resulting complex interactions with a lipophilic cell membrane, facilitating its uptake.[5,9] A short polyethylenglycol (PEG) moiety was also introduced in the vector structure by reaction of 1,1′,2-trisnorsqualenaldehyde[18] with 2,2′-ethylenedioxy bis(ethylamine) (Scheme 1), aiming to improve the colloidal stability, to reduce cytotoxicity and to modify the hydrophilicity without increasing the carrier/complex dimensions. Then, performing a Michael addition reaction of the resultant aminated derivative with *N*,*N*′-bis(acryloyl)cystamine (Scheme 1), a bioreducible disulfide linkage was inserted, to provide higher transfection efficiency primarily by facilitating intracellular trafficking.[9,19] Coupling the disulfide-based Sq sequence and LMWPEI, improvements in terms of transfection efficacy and cytocompatibility were envisaged by taking into account the self-assembling ability of the bioreducible, amphiphilic and water-soluble lipopolymer. The cumulation of an increased number of LMWPEI chains by aggregation is expected to give rise to a higher DNA compaction capacity coupled with a proton sponge effect and reduced cytotoxicity.[20] Cell and nucleus membrane penetrations are important tasks for a high transfection efficiency. Solutions to facilitate them in order to mediate intracellular delivery of the carrier cargo refer to the integration in the vector structure of cell penetrating peptides (CPP), conjugation with oligoarginine, or simple guanidinylation.[9,21,22] Herein, ^{1}H-pyrazole-1-carboxamidine hydrochloride was the reactant chosen for transformation of an appropriate amount of amino groups from the BPEI moiety to the guanidino groups.[21–23] With the aim of using and evaluating such vectors for the development of a gene-activated scaffold platform, Sq-BPEI-NH_2 labeling *via* 5-fluorescein isothiocyanate (Sq-BPEI-FITC, Scheme 1) was performed using a simple method adapted from the literature.[24]

Spectral data (^{1}H-NMR, ^{13}C-NMR, FT-IR) confirmed the successful development of the three Sq-BPEI based conjugates and of all their intermediates (Fig. 1, 2, S1, S2 and Table S1†).

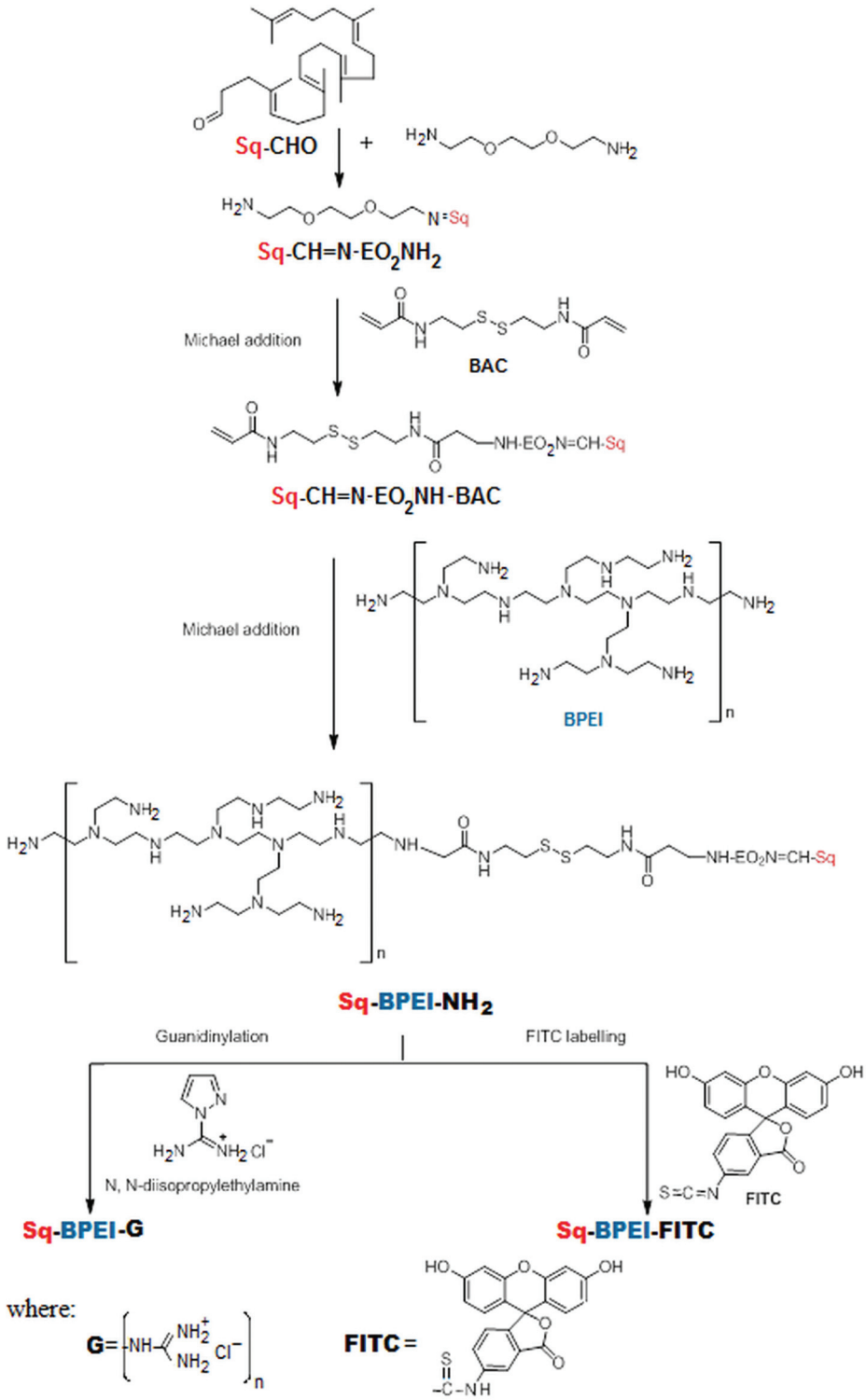

Scheme 1 Synthetic routes for three water-soluble amphiphilic conjugates: Sq-BPEI-NH_2 and its guanidinylated (Sq-BPEI-G) and labeled (Sq-BPEI-FITC) derivatives.

The transformation of the initial 1,1′,2-trisnorsqualenaldehyde to the Schiff-base by interaction with 2,2′-ethylenedioxy bis(ethylamine) was proved by the disappearance of the specific signals for the formyl group–situated at 9.75 ppm in the ^{1}H-NMR spectrum (Fig. 1), at 202.7 ppm in the ^{13}C-NMR registration, and at 2715 cm^{-1}/1728 cm^{-1} (ν_{CH} and $\nu_{C=O}$, respectively, from saturated aldehyde) in the FT-IR analysis (Fig. S1a, S2a, Table S1†); these were replaced by specific

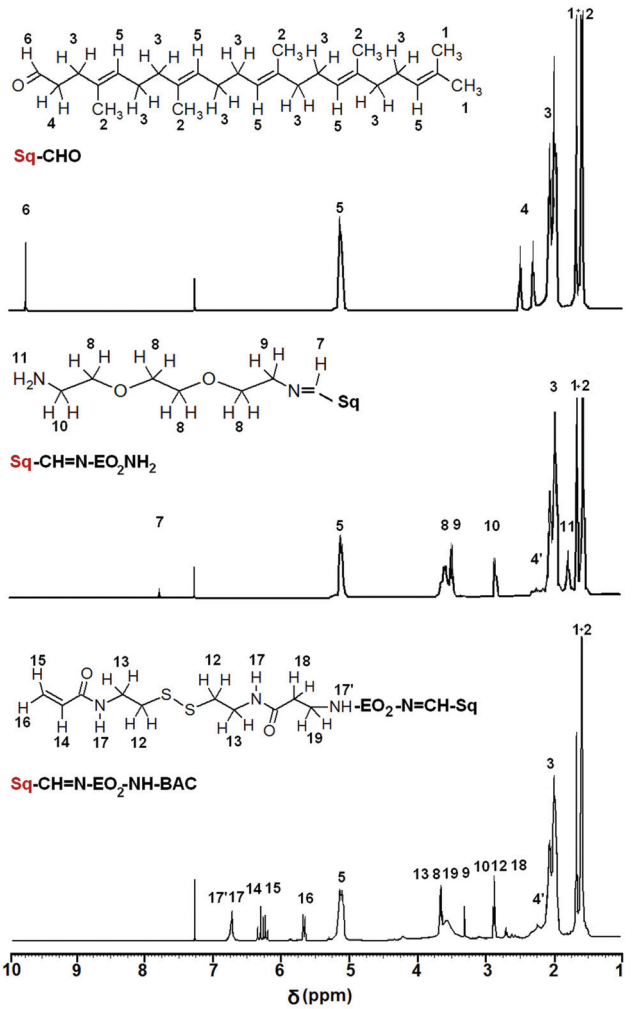

Fig. 1 ^{1}H-NMR spectra of the Sq-BPEI intermediates ($CDCl_3$).

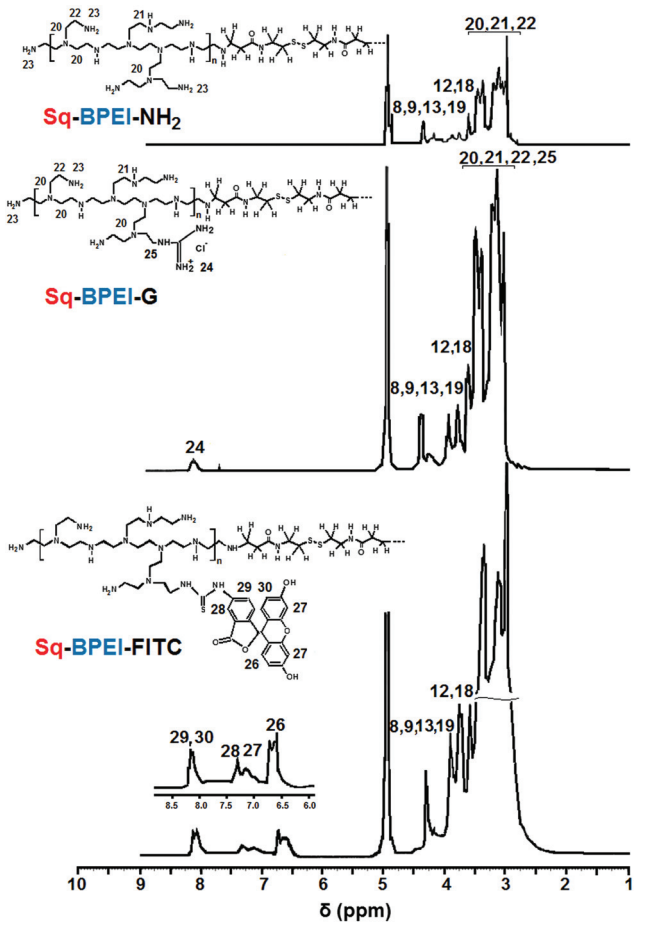

Fig. 2 ^{1}H-NMR spectra for the compounds obtained by Sq-BPEI-NH_2 functionalization (D_2O).

iminic group signals, situated at 8 ppm, 167 ppm (C═N) and 1573 cm^{-1}, respectively. The presence of the CH_2–O group is also easily observed as the attributed signals are situated at 3.4–3.7 ppm, 71 ppm and 1111 cm^{-1}. Further modification with *N*,*N*′-bis (acryloyl)cystamine is evidenced primarily by the inclusion of new signals in the registered spectra, attributable to amide (6.75 ppm, 74 ppm and 164 ppm) and vinyl group (5.70–6.35 ppm, 124 ppm, 129 ppm, 3066 cm^{-1} and 1620 cm^{-1}). The relative integration ratios of the specific ^{1}H-NMR signals (Fig. 1) in connected 2,2′-ethylenedioxy bis (ethylamine) (**8 and 9**) and BAC moieties (unreacted acryloyl groups–**14, 15, and 16**) to the signal attributed to methine groups in Sq (**5** in Fig. 1, situated at 5.03–5.13 ppm) were calculated to confirm that the reaction proceeded completely.

Once the BPEI moiety was added, the bands assignable to amine, imine groups and methylenic groups connected to them became predominant, while some of the other signals are shielded (amphiphilic compound). However, guanidinylation and labeling with FITC could be evidenced in the ^{1}H-NMR spectra (Fig. 2) by the appearance of characteristic signals in the 6.5–8.5 ppm range, while the retention of squalene and other moieties was confirmed from the FT-IR data (Fig. S2, Table S1†).

As observed from TEM, the resultant Sq/BPEI amphiphilic compounds with a hyperbranched structure may gradually aggregate in water to form discrete and large assemblies with the highest dimensions less than 200 nm (Fig. 3). The recorded morphology suggests the generation of multimolecular micelles. The amplified photos (Fig. S3†) clearly indicate a

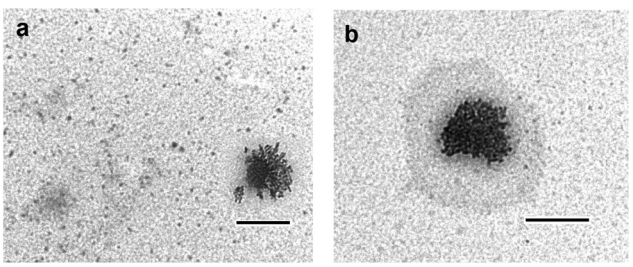

Fig. 3 TEM images for the aqueous solutions of samples (a) Sq-BPEI-NH_2 and (b) Sq-BPEI-G. Scale bar: 200 nm.

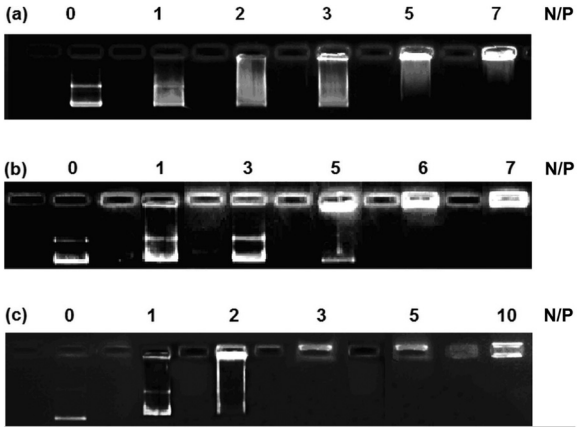

Fig. 4 Agarose gel electrophoresis registrations for the Sq/PEI developed carriers as compared to the used naked BPEI (1.8 kDa): (a) BPEI; (b) Sq-BPEI-NH_2; (c) Sq-BPEI-G. Lane 0: naked DNA. Lanes 1–10: complexes with the corresponding N/P ratios.

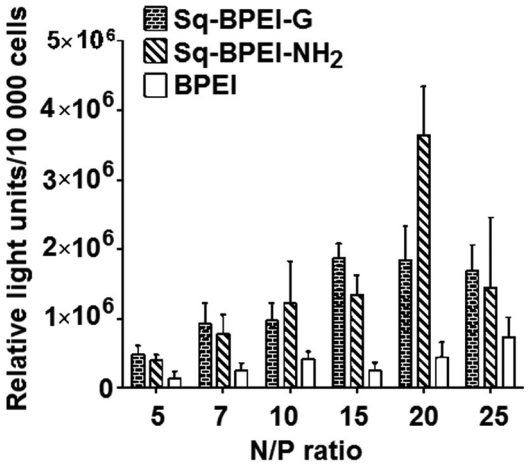

Fig. 5 Comparative representation of Luciferase assay data on HeLa cells (48 hours post transfection) performed in the presence of pLuc polyplexes with the studied gene carriers, at different N/P ratios.

fine structure; the large aggregates are composed of mostly spherical nanosized building units (5–15 nm). It is easy to observe the nanometric building units (probably unimolecular micelles as reported before for hyperbranched copolymers[25]) in a large number around the self-assembling larger structures.

For gene delivery, the complexation ability of the carrier with DNA and the vector/DNA ratio are critical design parameters to control both transfection efficiency and cytotoxicity. The ability of Sq-BPEI-NH_2 and Sq-BPEI-G to condense salmon DNA (SDNA) for cellular uptake was determined by agarose gel electrophoresis and compared with that of the branched LMWPEI used in their synthesis. Complete complexation was achieved for all polymers. As shown in Fig. 4, the DNA compaction ability decreases in the following order: Sq-BPEI-G $\gg$ Sq-BPEI-NH_2 > BPEI (1.8 kDa). In general, the transfection efficiency depends on the vector structural characteristics and on its concentration and it increases with the N/P ratio. To enhance the transfection efficacy, higher N/P ratios are required with the free carriers facilitating the cellular uptake as well as the intracellular trafficking.[26] Herein, the optimal transfections for HeLa cells were revealed (by confocal microscopy observation and Luciferase assay at 48 h post transfection) at N/P ratios of 15 for Sq-BPEI-G and of 20 for Sq-BPEI-NH_2 (Fig. S4 and 5), using a plasmid pGFP encoding, a variant of green fluorescent protein, and pLuc encoding luciferase. In addition, high luciferase expression was also observed after 48 h transfection in cell line HEK 293T with complexes of the two gene-vectors synthesized herein for the obtained optimum N/P ratios (Fig. S5†). It should be noted that the studied Sq/BPEI derivatives were able to transfect HeLa cells *in vitro* with transfection efficiencies significantly higher than those of the used LMWPEI. Thus, for N/P = 15, Sq-BPEI-G has a transfection efficiency 8.33 times higher than BPEI (1.8 kDa), while for N/P = 20, the Sq-BPEI-NH_2 based system achieves the highest transfection efficiency–one order of magnitude higher than that of BPEI. As expected, modification by guanidinylation highly improved carrier performances (*i.e.*, transfection efficiency) by decreasing inter-particle aggregation and by facilitating cell membrane penetration and intracellular trafficking. The lipidic moiety self-assembly, giving rise to increased local accumulation of LMWPEI chains, also contributed to the differences between the results obtained with the new carrier as compared to naked BPEI.

Biocompatibility is a vital factor for the application of gene transfection vehicles in humans. The *in vitro* cytotoxicity of the synthesized gene carriers was evaluated by MTS assay performed on HeLa cells in the presence of their polyplexes at different N/P ratios. As can be observed from the present data (expressed as a percentage of living cells in the samples containing polyplex, treated for 48 h, relative to the untreated cells– Fig. 6), the viability is higher than 90% and similar for the investigated vectors for a N/P ratio in the range of 10 to 15.

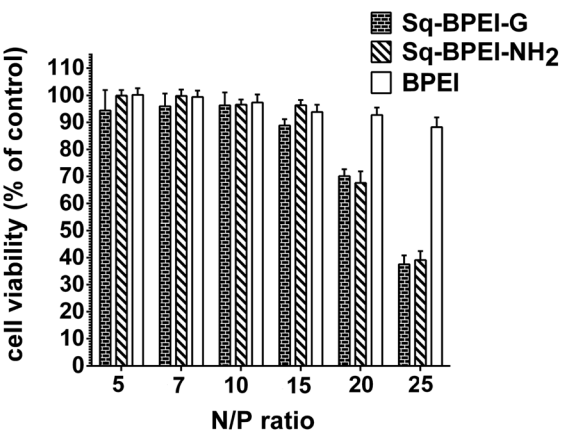

Fig. 6 Comparative cytotoxicity profiles of polyplexes formed with BPEI, Sq-BPEI-NH_2 and Sq-BPEI-G, respectively (MTS assay).

Design of combined non-viral gene delivery systems based on Sq/BPEI developed gene vectors and bioinspired scaffold

Compared to the traditional delivery methods, matrix mediated gene transfer strategy is considered to enhance gene delivery, increase the extent and duration of transgene expression and insure a safe profile for gene therapy.[15–17,27] Controlled release and the final transfection efficacy depend on the gene carrier design, the genetic material incorporation technique, specific interactions between the two (vector/scaffold) components (their formulation, topology, morphology) and scaffold degradation kinetics, which modulate the *in vitro* DNA release rate.[17,27] In a previous study, we reported the synthesis of a bioinspired hybrid cryogel, containing natural/synthetic polymers (atelocollagen, hyaluronic acid derivative, and poly(ε-caprolactone)), and polyethylenimine functionalized nano-hydroxyapatite ($CH_{10}P_{10}/HAp_{25}$-15) to be used as a 3-D matrix for encapsulation of polyplexes formed between BPEI (25 kDa) as a gene delivery vector and plasmid pDNA. The data showed that the entrapment of polyplexes into the matrix provides an increased polyplex stability and a sustained high level of transgene expression for at least 22 days together with reduced cytotoxicity as compared to free BPEI (25 kDa)/pDNA polyplexes.[14] In this context, the new Sq/BPEI gene-delivery vectors were subjected to loading in the mentioned hybrid cryogel $CH_{10}P_{10}/HAp_{25}$-15. In addition, the incorporation efficiency of polyplexes, the release kinetics of DNA and the transfection efficiency of the resulting combined systems were thoroughly studied to evaluate their performances and to find cues to control them. As revealed by SEM investigation (Fig. 7) and EDX data (see Table 1, N and P content modification), the polyplexes can be easily included in the macroporous hybrid matrix. Due to the high functionality of the hybrid cryogel, the polyplex can be immobilized by non-covalent interactions not only at the scaffold surface, but also inside the pores (Fig. 7b and c) by simple cryogel immersion in the aqueous polyplex dispersion.

To evaluate the transfection efficiency of the designed combined systems, the Sq-BPEI-NH_2/pEYFP (N/P = 20) and Sq-BPEI-G/pEYFP (N/P = 15) polyplexes, obtained for a fixed amount of pDNA (15 μg), were loaded in $CH_{10}P_{10}/HAp_{25}$-15 hybrid scaffold (pieces of ~1.0 mg) by hydrating the cryogel in the cell culture medium containing them; the 3D matrix was placed above the HEK 293T cells. As shown in Fig. 8, the expression of fluorescent protein could be observed after 24 h of cells exposure to polyplex-loaded matrices. It increased for both types of Sq/BPEI conjugates at 48 h and reached a maximum level at day 5. Continuing the experiment by splitting the cells every week in the presence of polyplex-loaded matrices, it was observed that the expression of fluorescent protein was maintained at a significant level up to day 26 (Fig. 8). A high level of transfection was observed in the cells underneath the matrices as compared to the cells in a remote field.

Table 1 Composition of the matrix before and after incorporation of Sq-BPEI-NH_2/SDNA polyplex (EDX data)

	At (%)	
Element	$CH_{10}P_{10}/HAp_{25}$-15	Sq-BPEI-NH_2/SDNA : $CH_{10}P_{10}/HAp_{25}$-15
C	62.02	61.07
N	13.83	15.66
O	21.66	19.36
Si	0.10	0.11
P	0.93	1.20
Ca	1.44	1.51

In an attempt to find biomimetic cues for scaffold design, earlier studies reported the achievement of temporal control of the transgene expression profile by the spatial distribution of polyplexes within a sphere-templated fibrin scaffold;[28] different peak transfection was observed, which was related to the retention of PEI/DNA polyplexes on the surface of the interconnected pores in the scaffold, or to their embedding within biopolymer fibrils (later peak expression). Moreover, the specific polyplex-matrix interactions also influence the possible modulation of gene delivery profile by simply modifying the scaffold composition, which was proved recently.[29] Considering our earlier data[14] the specific degradation of the scaffold used herein (rate, mechanism, and composition modification) may also interfere with the architecture and composition effects to determine the timing of the highest level transfection for the investigated systems due to spatial and temporal gradients of mass transfer.

To evaluate the biocompatibility of the developed combined systems, we investigated the morphology of the cells during

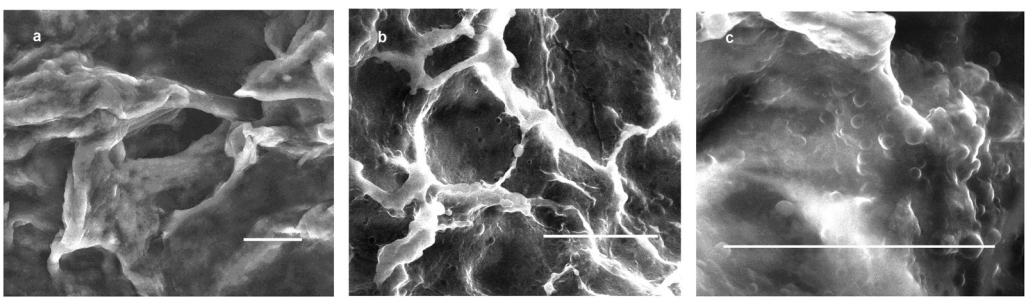

Fig. 7 SEM microphotographs for the hybrid matrix (a) before and (b, c) after loading with Sq-BPEI-FITC/SDNA polyplexes. Bar: 20 μm.

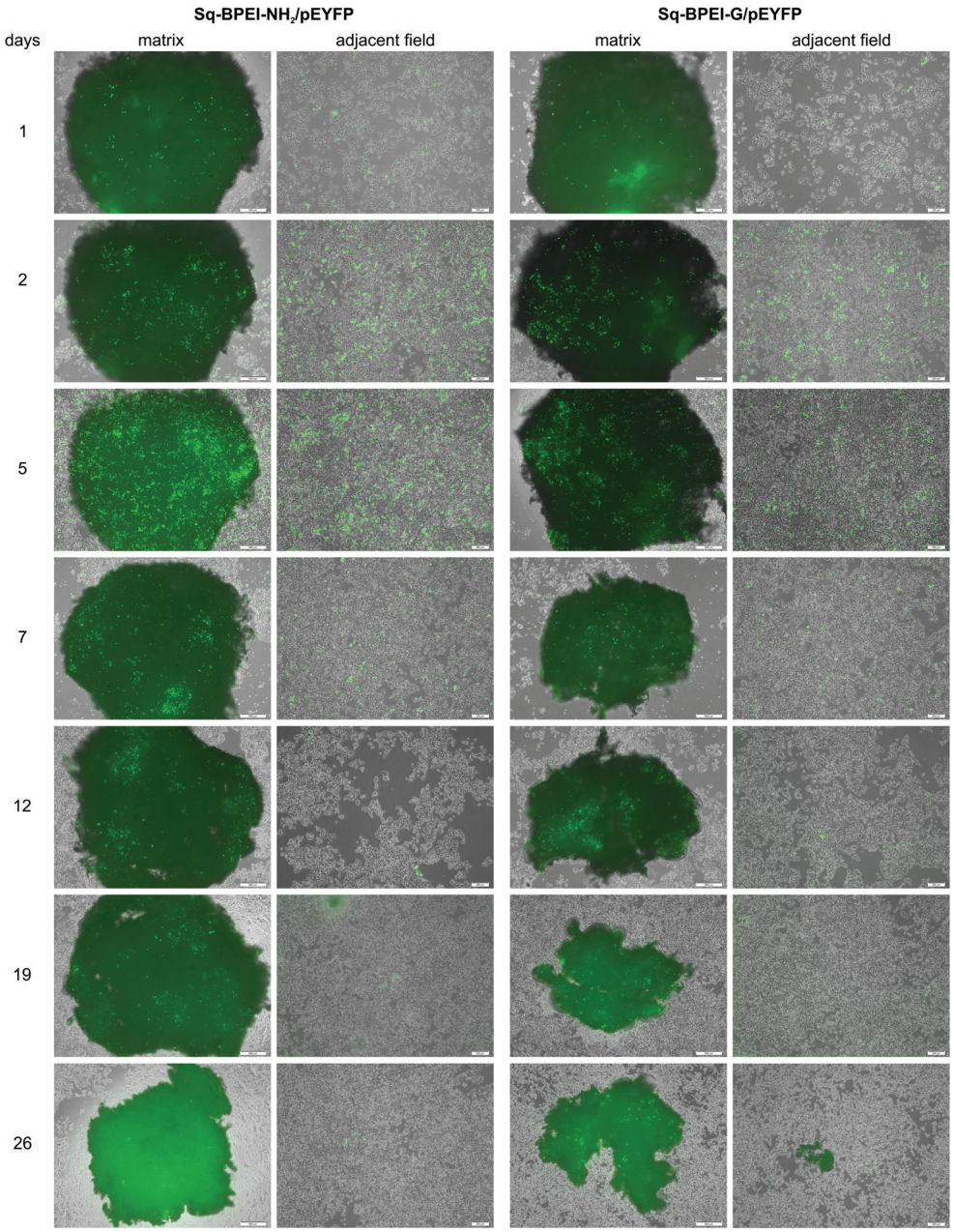

Fig. 8 Fluorescent protein expression in HEK 293T cells incubated in the presence of Sq-BPEI-NH_2/pEYFP (N/P = 15) and Sq-BPEI-G/pEYFP (N/P = 20) polyplexes embedded in $CH_{10}P_{10}/HAp_{25}$-15 matrix. Bar: 500 μm (for images containing matrices) and 200 μm (for images taken for a remote field).

the experiment as well as the cells incubated in the presence of polyplexes (pEYFP – Sq/BPEI conjugates), free or embedded into matrices, as compared to that of control cells or cells exposed to free plasmid (Fig. S6†). No essential differences could be observed. It is to be mentioned that earlier data showed that the degradation products released after 24 h from the plain matrix or pDNA loaded matrix show a decrease of cell viability up to about 60%.[14] However, cell viability regained normal/acceptable values (over 85%) after 72 h. A significant reduction in the cytotoxicity was registered for BPEI (25 kDa)/pDNA when loaded in the $CH_{10}P_{10}/HAp_{25}$-15 matrix. These data suggest a good cytocompatibility of the investigated systems.

To gain more insight into the mechanism of DNA transfer from the substrate, further studies were performed by examining SDNA and vector release from the combined systems by means of UV-Vis (for SDNA) and fluorescent spectrophotometry (for labeled carrier Sq-BPEI-FITC). The experiments were performed in static and dynamic conditions (samples disposed on a temperature controlled shaker, 200 rpm, aiming to mimic the cell motility). As shown in Fig. 9, the release kinetics was better controlled when polyplexes were used instead of

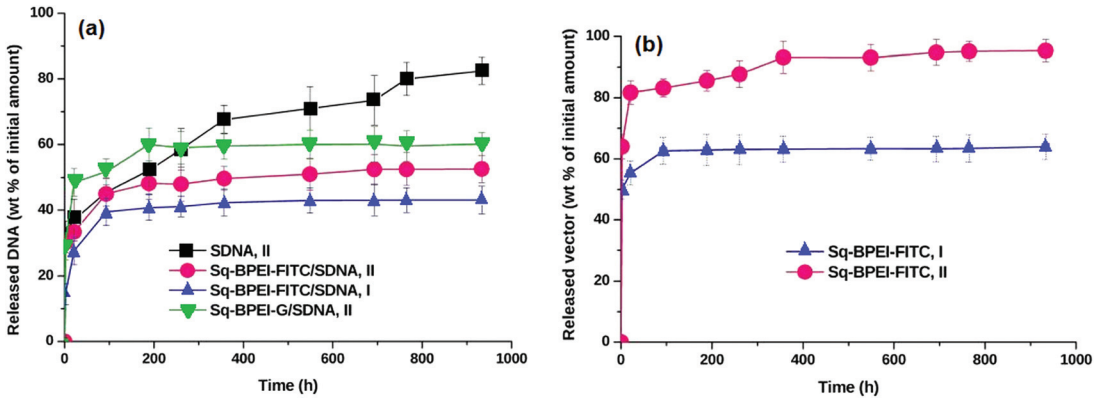

Fig. 9 Quantitative cumulative release evaluation over time of (a) SDNA (wt% of total loaded SDNA as naked SDNA or polyplex with Sq/BPEI based vectors) and (b) vector (wt% of total vector amount loaded as polyplex with Sq-BPEI-FITC) incorporated in the hybrid cryogel $CH_{10}P_{10}/HAp_{25}$-15. Conditions: (I) static (sample maintained at 37 °C in oven) and (II) dynamic regime (samples on temperature controlled shaker, 200 rpm, 37 °C).

naked DNA. An initial burst DNA release is evident for all investigated systems, mostly in the first 2 h with an increased effect in the dynamic system. However, even the released naked SDNA amount with respect to the initial SDNA (33.6 wt%) is lower than that reported for combined systems comprising DNA and a matrix based on collagen only,[30,31] where it was situated between 60% and 80%, while herein, ~80% SDNA was released only after 1000 h. For the Sq-BPEI–FITC/SDNA polyplex, the rate of delivery lowered after about 100 h, while for the Sq-BPEI-G/SDNA system, the rate drastically decreased after 200 h. Thus, for all kinetic plots, an important slope change is observed in the 100–200 h time interval, and a plateau is reached after about 700 h (at 40–60% SDNA released relative to then initial amount) when the majority of the still existing polyplexes appear to remain associated to the scaffold. These aspects are directly related to the matrix degradation behavior as proved in an earlier study,[14] and the comparison of UV registrations for the SDNA release against matrix (as control sample) and pure water. They are ascribed primarily to the removal of high amounts of amorphous and subsequently organized biopolymers (crystalline protein and densely packed protein-glycosaminoglycan complex) from the hybrid 3D construct. The slope changes explain the maximum level for the expression of fluorescent protein after 5 days/120 h (Fig. 8), and a drastic diminishing after 26 days/624 h. Between the mentioned time limits (from 200 h to 700 h), some polyplex is still released, as evidenced in Fig. 9, for Sq-BPEI-FITC/SDNA under dynamic experimental conditions, which approximate better a biological system (*i.e.*, 9 wt% Sq/BPEI carrier and 5.5 wt% SDNA delivered in comparison with 0.5 wt% Sq/BPEI vector and 3.5 wt% SDNA for static conditions). The expression of the fluorescent protein at a sufficiently high level until day 26 may be due to, on the one hand, the shedding of polyplexes from the matrix over time and, on the other hand, the fact that the plasmids are partitioned to the daughter cells after cellular division. Therefore, fluorescent protein can be produced in the absence of new entry of polyplexes.

The comparison of the release profiles strongly suggests that they are related to specific van der Waals (electrostatic and hydrofobic) interactions, which are responsible for the adsorption of DNA and polyplexes[30–32] and their release control. Electrostatic repulsions appearing in the presence of Sq-BPEI-G might be the reason for the observed increase in desorption rate even when compared to naked DNA for the first 260 h. Thus, the complex matrix composition was efficient in promoting appropriate interactions between the encapsulants and the hybrid scaffold for an improved control over the release profile. From the presented data, it is evident that the release steps primarily depend on the carrier structure and the matrix degradation rate and in a limited measure, on the dynamic regime, which facilitates diffusion.

As found by gel electrophoresis investigations, the released DNA retained its structural integrity in most cases during the experiment (except the system based on the Sq-BPEI-G vector, after 600 h). For the combined system containing Sq-BPEI-FITC studied in static conditions, the DNA still remaining after 39 days (44 wt% SDNA delivered) was released in the medium containing sodium dodecyl sulphate (SDS), and could be recovered up to 96% (over an additional period of 6 days, following the experimental program).

Although the minimum N/P ratio for PEI to completely condense pDNA into polyplexes is known to be around 3, for the kinetics study, a N/P = 10 ratio was used, which is the optimum value according to literature[33–35] and the data reported here (DNA complexing ability of synthesized vectors, acceptable transfection efficiency and cytocompatibility). Thus, there are bound cationic chains involved in the complexation with DNA and free BPEI-based chains. Detailed earlier studies demonstrated that excess PEI chains (free PEI) favor polyplexes internalization by cells through clathrine mediated endocytosis (CME) and facilitate the intracellular trafficking, while the "proton sponge" effect was found to have no dominant effect.[35,36] Taking into account that a high amount of free PEI chains increases cytotoxicity, some authors successfully verified the possibility to reach high transfection efficiency by

adding PEI following polyplex formation with less toxic carriers.[37] In the present paper, by comparing the SDNA and carrier delivery kinetics plots (making use of the labeled Sq-BPEI–FITC derivative), it was evidenced that the burst release coresponds to the desorption of a large amount of excess free BPEI-based carrier retained on the matrix surface (see Fig. 7) together with the polyplex. The calculated N/P was found to be 34 in static conditions and about 21 in the dynamic ones after 2 h and about 20 after 21 h. However, after 100 h, the N/P ratios in the released gene-delivery system became about 16 in both static and dynamic experimental conditions. Similar data (not shown here) were also obtained for C60-BPEI-FITC synthesized in an earlier study.[38] It should be noted that the best SDNA packing with C60-PEI was obtained for N/P ratios higher than 5, and the maximum transfection efficiency for the C60-PEI/pEYFP polyplex was found at N/P ratios between 10 and 20. Most probably, the remaining DNA was retained in the hybrid matrix with some components (LPEI, residual atelocollagen *etc*.) being able to complex the DNA themselves. Thus, the excess PEI-based carrier may be optimized to a minimum level taking into account both vector and matrix characteristics. Further studies are required to better understand some of the delivery aspects mentioned in this study.

3. Conclusion

Aiming to develop gene-delivery systems with improved biocompatibility, biodegradability and transfection efficiency, new gene delivery carriers based on squalene and polyethylenimine were synthesized using 1,1′,2-trisnorsqualenaldehyde as a raw material by a simple route primarily employing Michael addition reactions. The obtained Sq/BPEI conjugates, namely Sq-BPEI-NH_2 and its guanidinylated derivative Sq-BPEI-G, were found to efficiently complex DNA. When used to transfect HeLa cells, the conjugates yielded maximum luciferase expression levels at N/P ratios of 20 for the Sq-BPEI-NH_2 based polyplex and 15 for the Sq-BPEI-G based polyplex, which were higher up to one order of magnitude as compared to the naked BPEI–based polyplex. The inclusion of the polyplexes formed with pEYFP in a hybrid cryogel ($CH_{10}P_{10}$/HAp_{25}-15) provided a sustained release of genetic material over about 26 days with a maximum expression on day 5 without any visible toxic effect on cells (experiment carried out on the HEK 293T cell line). Quantitative evaluation of SDNA and vector release from the 3D macroporous matrix in time evidenced a release kinetics control due to specific interactions (electrostatic and hydrophobic) between excess free carrier, polyplexes and the hybrid cryogel, in correlation with their structural characteristics and with the degradation of the porous matrix. Thus, the developed systems offer tunable genetic material release, long-term bioavailability and a relatively facile synthesis procedure. The earlier results and the results reported herein also point on good biocompatibility. Further studies are recommended for their application in gene-activated matrix (GAM) systems with pre-designed optimized performances.

Conflicts of interest

There are no conflicts of interest to declare.

Acknowledgements

This publication is part of a project that has received funding from the European Union's Horizon 2020 research and innovation programme under grant agreement No 667387 WIDESPREAD 2-2014 SupraChem Lab.

References

1 K. Lundstrom and T. Boulikas, *Technol. Cancer Res. Treat.*, 2003, **2**(5), 471–486.
2 D. W. Pack, A. S. Hoffman, S. Pun and P. S. Stayton, *Nat. Rev. Drug Discovery*, 2005, **4**(7), 581–593.
3 A. Elouahabi and J.-M. Ruysschaert, *Mol. Ther.*, 2005, **11**(3), 336–347.
4 S. M. Dizaj, S. Jafari and A. Y. Khosroushahi, *Nanoscale Res. Lett.*, 2014, **9**, 252–260.
5 L. Jin, X. Zeng, M. Liu, Y. Deng and N. He, *Theranostics*, 2014, **4**(3), 240–255.
6 Y. Xiang, N. N. L. Oo, J. P. Lee, Z. Li and X. J. Loh, *Drug Discovery Today*, 2017, **22**(9), 1318–1335.
7 U. Lungwitz, M. Breunig, T. Blunk and A. Göpferich, *Eur. J. Pharm. Biopharm.*, 2005, **60**(2), 247–266.
8 H. Lv, S. Zhang, B. Wang, S. Cui and J. Yan, *J. Controlled Release*, 2006, **114**(1), 100–109.
9 T. Wang, J. R. Upponi and V. P. Torchilin, *Int. J. Pharm.*, 2012, **427**(1), 3–20.
10 S. Han, R. I. Mahato and S. W. Kim, *Bioconjugate Chem.*, 2001, **12**(3), 337–345.
11 V. Allain, C. Bourgaux and P. Couvreur, *Nucleic Acids Res.*, 2012, **40**(5), 1891–1903.
12 C. Gehin, J. Montenegro, E.-K. Bang, A. Cajaraville, S. Takayama, H. Hirose, S. Futaki, S. Matile and H. Riezman, *J. Am. Chem. Soc.*, 2013, **135**(25), 9295–9298.
13 L. Clima, D. Peptanariu, M. Pinteala, A. Salic and M. Barboiu, *Chem. Commun.*, 2015, **51**(99), 17529–17531.
14 B. C. Simionescu, M. Drobota, D. Timpu, T. Vasiliu, C. A. Constantinescu, D. Rebleanu, M. Calin and G. David, *Mater. Sci. Eng., C*, 2017, **81**, 167–176.
15 J. Bonadio, *Adv. Drug Delivery Rev.*, 2000, **44**, 185–194.
16 O. Bleiziffer, E. Eriksson, F. Yao, R. E. Horch and U. Kneser, *J. Cell. Mol. Med.*, 2007, **11**(2), 206–223.
17 E. G. Tierney, G. P. Duffy, S.-A. Cryan, C. M. Curtin and F. J. O'Brien, *Organogenesis*, 2013, **9**(1), 22–28.
18 E. Lepeltier, B. Loretz, D. Desmaële, J. Zapp, J. Herrmann, P. Couvreur and C.-M. Lehr, *Biomacromolecules*, 2015, **16**, 2930–2939.
19 S. Bauhuber, C. Hozsa, M. Breunig and A. Göpferich, *Adv. Mater.*, 2009, **21**, 3286–3306.

20 M. Breunig, U. Lungwitz, R. Liebl and A. Goepferich, *Proc. Natl. Acad. Sci. U. S. A.*, 2007, **104**, 14454–14459.
21 L. A. Tziveleka, A. M. Psarra, D. Tsiourvas and C. M. Paleos, *J. Controlled Release*, 2007, **117**, 137–146.
22 C. V. Bonduelle and E. R. Gillies, *Pharmaceuticals*, 2010, **3**(3), 636–666.
23 M. S. Bernatowicz, Y. Wu and G. R. Matsueda, *J. Org. Chem.*, 1992, **57**, 2497–2502.
24 J.-H. Kim, S. Lee, K. Kim, H. Jeon, R.-W. Park, I.-S. Kim, K. Choi and I. C. Kwon, *Chem. Commun.*, 2007, **13**, 1346–1348.
25 H. Hong, Y. Mai, Y. Zhou, D. Yan and J. Cui, *Macromol. Rapid Commun.*, 2007, **28**, 591–596.
26 T. Xu, W. Liu, S. Wang and Z. Shao, *Int. J. Nanomed.*, 2014, **9**, 3231–3245.
27 C. Cam and T. Segura, *Curr. Opin. Biotechnol.*, 2013, **24**, 855–863.
28 J. M. Saul, M. P. Linnes, B. D. Ratner, C. M. Giachelli and S. H. Pun, *Biomaterials*, 2007, **28**, 4705–4716.
29 R. M. Raftery, E. G. Tierney, C. M. Curtin, S.-A. Cryan and F. J. O'Brien, *J. Controlled Release*, 2015, **210**, 84–94.
30 H. Cohen-Sacks, V. Elazar, J. Gao, A. Golomb, H. Adwan, N. Korchov, R. J. Levy, M. R. Berger and G. Golomb, *J. Controlled Release*, 2004, **95**, 309–320.
31 F. Scherer, U. Schillinger, U. Putz, A. Stemberger and C. Plank, *J. Gene Med.*, 2002, **4**, 634–643.
32 R. A. Hortensius, J. R. Becraft, D. W. Pack and B. A. C. Harley, *Biomater. Sci.*, 2015, **3**(4), 645–654.
33 Y. Yue, F. Jin, R. Deng, J. Cai, Y. Chen, M. C. Lin, H. F. Kung and C. Wu, *J. Controlled Release*, 2011, **155**(1), 67–76.
34 Y. Yue, F. Jin, R. Deng, J. Cai, Z. Dai, M. C. Lin, H.-F. Kung, M. A. Mattebjerg, T. L. Andresen and C. Wu, *J. Controlled Release*, 2011, **152**(1), 143–151.
35 Y. T. Ko, U. Bickel and J. Huang, *Oligonucleotides*, 2011, **21**(2), 109–114.
36 R. V. Benjaminsen, M. A. Mattebjerg, J. R. Henriksen, S. Moein Moghimi and T. L. Andresen, *Mol. Ther.*, 2013, **21**(1), 149–157.
37 L. J. C. Albuquerque, C. E. de Castro, K. A. Riske, M. C. Carlan da Silva, P. I. R. Muraro, V. Schmidt, C. Giacomelli and F. C. Giacomelli, *Biomacromolecules*, 2017, **18**(6), 1918–1927.
38 C. M. Uritu, C. D. Varganici, E. L. Ursu, A. Coroaba, A. Nicolescu, A. I. Dascalu, D. Peptanariu, D. Stan, C. A. Constantinescu, V. Simion, M. Calin, S. S. Maier, M. Pinteala and M. Barboiu, *J. Mater. Chem. B*, 2015, **3**(12), 2433–2446.